Zhao, T, Zhao, C, Zhang, JF, Mitrovic, IZ, Lim, EG, Yang, L, Song, T and Zhao, C

Enhancement on the performance of eco-friendly solution-processed InO/AlO thin-film transistors via lithium incorporation

Article

Citation (please note it is advisable to refer to the publisher's version if you intend to cite from this work)

Zhao, T, Zhao, C, Zhang, JF, Mitrovic, IZ, Lim, EG, Yang, L, Song, T and Zhao, C (2020) Enhancement on the performance of eco-friendly solution-processed InO/AlO thin-film transistors via lithium incorporation. Journal of Alloys and Compounds, 829. ISSN 0925-8388

Performance Enhancement of Eco-friendly Solution Processed InO/AlO Thin-film Transistors via Li incorporation

T. S. Zhao, C. Zhao, J. F. Zhang, I. Z Mitrovic, E. G. Lim, L. Yang, S. C. Yu and C. Z. Zhao

***Abstract*— Solution based fabrication of thin film transistors (TFTs) has low cost and roll-to-roll capability. Indium oxide is one of the promising materials for metal oxide semiconductor layer in TFTs. Early works used high temperature (~700 °C) anneal, which is not suitable for flexible substrates. The toxic solvents, such as 2-methoxyethanol (2-Me), have been widely used in the preparation of precursor solutions. To overcome these challenges, we propose a low temperature (≤ 250 ℃) and eco-friendly process through incorporation of Lithium. Both X-ray photoelectron spectroscopy and electrical characterizations were carried out to optimize the process. The best result was obtained with 10 at.% Lithium incorporation. The high field effective mobility, averaged over 30 devices, is 21.6 $cm^2·V^{-1}·s^{-1}$, which is 2~4 times of that reported by early works for low temperature solution prepared InO films. They were used to build an inverter successfully. This eco-friendly solution process has the potential for low cost fabrication of TFTs on flexible substrate.**

***Index Terms*— high-*k* materials, InO, solution process, TFT**

I. INTRODUCTION

Owing to its potential for large-area fabrication, equipment simplicity, roll-to-roll capability, atmospheric processing, and low-cost, the solution process has attracted many attentions, especially for fabricating metal oxide thin-film transistors (MOTFTs) [1-3]. Among various metal oxides, indium oxide (InO) is a promising semiconductor due to its high carrier mobility, a wide band gap (3.6-3.75 eV), and a superb transparency in visible region [4, 5]. These advantages make the solution-processed InO a promising candidate for fabricating high-performance MOTFTs.

Early work fabricated InO film with good quality through a high-temperature (~700 °C) annealing, which gives the critical energy crest for 1) dissociation, 2) solid-state structural integrity (condensation and densification), and 3) impurity removal for metal−oxygen−metal (M−O−M) lattice formation [6]. There is a trade-off between the annealing temperature and the film quality. Lowering temperature leads to an increase of oxygen vacancy (V_o) and metal-hydroxyl (M-OH) bonds, which possibly act as traps in the film. Since high temperature process is not suitable for fabricating MOTFT on flexible substrates, there is a need to develop new low temperature process. Another problem with the solution based fabrication of MOTFTs is the use of toxic solvents such as 2-methoxyethanol (2-Me) in preparing precursor solutions [7, 8].

The objective of this work is to tackle these challenges by developing an eco-friendly low temperature (<300 °C) process. It has been reported that hydrogen concentration in the film could be suppressed by akali metal ions [9, 10]. Lithium incorporation is used here to reduce the V_o and M-OH bonds. Deionized water (DI water) has better solubility for indium nitrate ($In(NO_3)_3$), lower molar mass, and lower boiling point (100 °C) than 2-Me (>130 °C). Its potential as an eco-friendly solvent is explored in this work.

Compared with the solution processed Indium-based TFTs reported by recent works [11-15], the mobility of TFTs fabricated by the process proposed and optimized in this work is 2~4 times higher (Table I). The TFTs were used to build inverters successfully. Finally, their reliability was tested under positive gate bias (PGB) stresses and the instability mechanism was analyzed.

TABLE I
RECENT REPORTS OF SOLUTION PROCESSED INDIUM BASED TFTS

Semiconductor	Temp. (℃) /Solvent	Mobility ($cm^2·V^{-1}·s^{-1}$)	Year	Ref.
InO	260/DI water	6.67	2018	[11]
InO	600/2-Me	5.61	2017	[12]
InO	200/2-Me	≈5	2016	[13]
InZnSnO	400/DI water	14	2016	[14]
InO	250/DI water	10.78	2016	[15]
Li-InO	250/DI water	Average 21.6	This work	

II. EXPERIMENTAL

The AlO precursor solution was prepared by dissolving 0.6 M aluminum nitrate nonahydrate ($Al(NO_3)_3·9H_2O$, Aladdin) in DI water. 7.5 M hydrogen peroxide (H_2O_2, Aladdin) was added

This research was funded in part by the National Natural Science Foundation of China (21503169, 2175011441, 61704111), Key Program Special Fund in XJTLU (KSF-P-02, KSF-A-04, KSF-A-05, KSF-T-03).*(Corresponding author: Chun Zhao)*

T. S. Zhao, C. Zhao, C. Z. Zhao, E.G. Lim and S.C. Yu are with the Department of Electrical and Electronic Engineering, Xi'an Jiaotong-Liverpool University, Suzhou, China. (e-mail: Chun.Zhao@xjtlu.edu.cn).

J. F. Zhang is with the Electrical Electronic Engineering Research Centre, Liverpool John Moores University, Liverpool, UK.

I. Z. Mitrovic is with the Department of Electrical Engineering and Electronics, University of Liverpool, Liverpool, UK.

L. Yang is with the Department of Chemistry, Xi'an Jiaotong-Liverpool University, Suzhou, China.

to reduce the defects in the dielectric layer. The InO precursor solution was prepared by dissolving 0.1 M indium nitrate hydrate ($In(NO_3)_3{\cdot}xH_2O$, Aladdin) in DI water. Different Li concentrations (0, 5, 10%, and 15 at.%) were obtained by dissolving 0, 0.005, 0.01, and 0.015 M lithium acetate ($LiOOCCH_3$, Aladdin) in the InO precursor solution, respectively. The solutions were ultra-sonically cleaned and filtered.

For TFTs, Fig. 1 shows that the AlO precursor solution was spun onto the heavily doped silicon substrates to prepare the dielectric layer. After that, the InO precursor solutions were spun onto the surface of AlO layer, followed by annealing at 250 °C under ambient atmosphere for 1 hour. This temperature was selected based on the thermogravimetric analysis (TGA) and differential thermal analysis (DTA) in Fig. 2(f). It clearly shows that the solvent residues for aqueous based solution can be effectively removed at a temperature of 250 ℃ or above, which is consistent with the previous reports [16, 17]. 250 ℃ is a good trade-off between the physically stable thin films and a low thermal budget, therefore.

The Al source and drain electrodes were deposited onto the semiconductor layer through a shadow mask with a Width/Length ratio of 15.

III. RESULTS AND DISCUSSION

To investigate the impact of Li incorporation on the chemical bonding states and compositions of InO layers, the X-ray photoelectron spectra (XPS) were measured and plotted in Figs. 2(a) to (e). The O 1s XPS spectra can be divided into three sub-peaks through deconvolution. They are centered at 529.8, 531.0, and 531.8 eV, which correspond to the M-O bonds, the O^{2-} ions near oxygen vacancy (V_o), and the M-OH bonds, respectively [17, 18]. M-O bonds enable stable conductive channel, while the V_o and M-OH bonds induce positive ions that act as donor-like traps under the application of gate bias [19]. The more M-O bonds and the less V_o and M-OH bonds, the better, therefore.

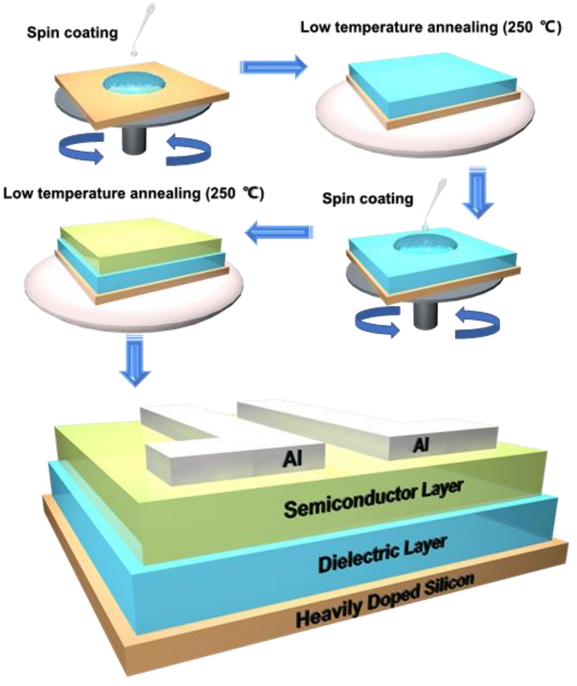

Fig. 1. Schematic diagrams of the fabrication process flow.

The intensity of M-O peaks (centered at 529.8 eV) increases with Li^+ concentration and reaches a maximum of 67.1 % at 10 at.% Li. This phenomenon could be attributed to Li assisting the formation of In-O network [11]. Excessive doping of Li to 15 at.%, however, has an adverse effect: an increase of M-OH peak and a decrease of M-O peak. This can be mainly attributed to the increase in lithium hydroxide (LiOH) and the degradation of InO microstructure [10]. As a result, 10 at.% Li incorporation is the optimal condition.

Fig. 3(a) shows the transfer characteristics of Li-InO/Al_2O_3 TFTs with Li at 0, 5, 10, and 15 at.%, respectively. Fig. 3(b) gives the output characteristics under different Vg for TFTs with 10 at % Li. They exhibit convincing n-channel field effect transistor characteristics. Drain voltage in Fig. 3(b) was swept in both directions and hysteresis is negligible. Their key properties are summarized in Table II, which are the average values of 30 devices. The samples with 10 at.% Li incorporation have the highest mobility of 21.6 $cm^2{\cdot}V^{-1}{\cdot}s^{-1}$, the lowest subthreshold swing (S.S.) of 0.25 V/dec, a V_{th} of 0.5 V, and an on/off current ratio of approximately 10^4. This agrees with the interpretation that M-O bonds benefit the TFT's performance, while the V_o and M-OH bonds degrade it.

As Li concentration reaches 15 at.%, the on/off ratio is reduced significantly to less than 1000. The devices can no longer be switched off properly and the leakage current increased by over one order of magnitude. It appears that there is a limit for the Li incorporation into InO. Once this limit is

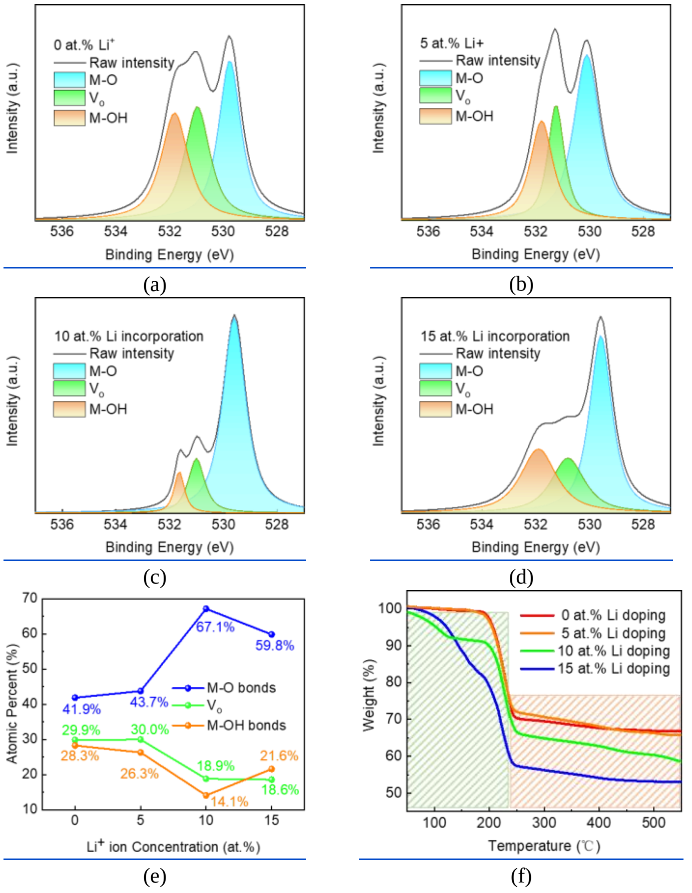

(a) (b)

(c) (d)

(e) (f)

Fig. 2. XPS spectra of (a) 0 at.%, (b) 5 at.%, (c) 10 at.%, and (d) 15 at.% Li doped samples. (e) Atomic percentage of M-O bonds, V_o, and M-OH bonds at different Li concentrations. (f) TGA results of InO with different Li concentrations.

reached, the excessive Li introduces defects in the film [20]. They cause a resistor-like conduction between source and drain, which is not controlled by the gate.

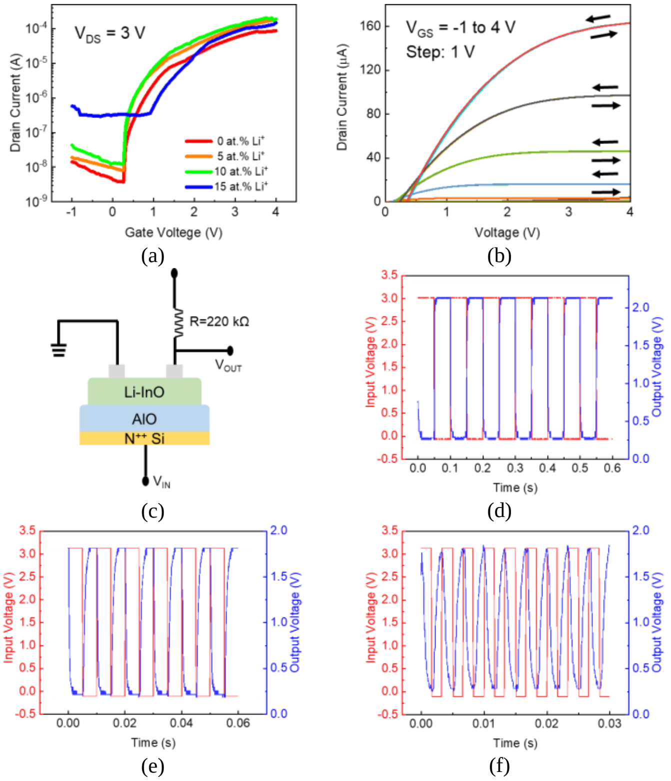

Fig. 3. (a) Transfer characteristics of 0, 5, 10, and 15 at.% Li incorporated samples. (b) Output characteristics of 10 at.% Li doped samples. (c) An inverter by connecting a 10 at.% Li-InO/AlO TFT with a 220 kΩ external resistor. Dynamic measurements of the inverter at (d) 10 Hz, (e) 100 Hz, and (f) 300 Hz.

To explore the applications of the TFTs in circuits, a resistor-loaded inverter was built by connecting the 10 at.% Li incorporated In_2O_3/Al_2O_3 TFTs in series with a 220 kΩ resistor, as illustrated in Fig. 3(c). The dynamic behavior of the inverter was measured with an input voltage of a square waveform at 10, 50, 100, and 300 Hz, respectively. Figs. 3(d)-(f) show that the output voltage has the inverter-like on/off states up to 300 Hz. This compares well with the sub-10 Hz reported by recent works [11, 21].

TABLE II

ELECTRICAL PROPERTIES OF LI-INO/ALO TFTS

Li concentration (at.%)	Mobility ($cm^2 \cdot V^{-1} \cdot s^{-1}$)	S.S. (V/dec)	V_{th} (V)	On/off Ratio
0	4.5	0.35	0.8	~10^4
5	17.3	0.28	0.6	~10^4
10	21.6	0.25	0.5	~10^4
15	19.2	1.03	1.4	~400

To investigate the reliability of the TFTs with Li incorporation, a 1000 s positive gate bias (PGB) stress was applied on the samples with 10 at.% and without Li incorporation. As shown in Fig. 4(a), the V_{th} of the devices without Li incorporation had shifted by 1.3 V, while the ones with 10 at.% incorporation had shifted only by 0.85 V along the negative direction. The V_{th}-stability is improved by 35% through Li incorporation, therefore.

For a bottom-gate n-channel TFT, once the bias applied on bottom gate has reached the V_{th}, a conductive channel is formed by the electrons near the dielectric layer (the small-blue dots in Fig. 4(b)). Under PGB stress, the V_o and M-OH bonds in the bulk of semiconductor can become positively charged (the big-red dots in Fig. 4(b)). These positive charges effectively act as an extra positive "top gate" bias, which assists the formation of the conductive channel [19]. As a result, the V_{th} of bottom gate shifts negatively. The Li-incorporation reduces the amount of V_o and M-OH bonds, weakens the effect of "top gate", and improves the V_{th}–stability.

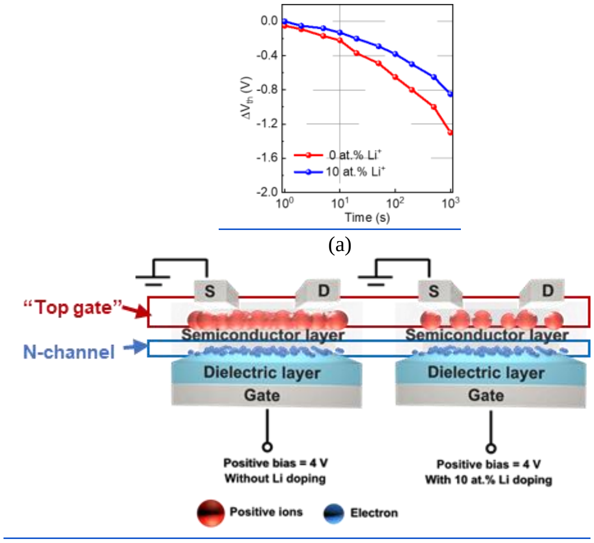

(b)

Fig. 4. (a) V_{th} shifts under PGB stress of the InO/AlO TFTs with/without 10 at.% Li-incorporation. (b) The microscopic schematic of channel layers with/without Li-incorporation under PGB stress.

IV. CONCLUSION

In this work, we have presented a fully solution-processed fabrication scheme for Li-incorporated InO/AlO thin-film transistors using an eco-friendly solvent. The effects of Li concentration were studied through both physical and electrical characterizations and the optimal level is found to be 10 at.%. The XPS results suggest that Li^+ ion incorporation assists in forming a strong InO network. The low temperature InO TFTs were successfully fabricated with a mobility of 21.6 $cm^2 \cdot V^{-1} \cdot s^{-1}$, threshold voltage of 0.5 V, subthreshold swing of 0.25 V/dec, and on/off ratio of ~10^4, averaged over 30 samples. A resistor-loaded inverter was demonstrated with a frequency up to 300 Hz.

V. REFERENCE

[1] Y. Chen, W. Huang, and V. K. Sangwan, "Polymer Doping Enables a Two-Dimensional Electron Gas for High-Performance Homojunction Oxide Thin-Film Transistors," *Adv. Mater.*, 31.4 (2019): 1805082.

[2] W. Cai, S. Park, J. Zhang and J. Wilson, "One-Volt IGZO Thin-Film Transistors With Ultra-Thin, Solution-Processed Al x O y Gate Dielectric," *IEEE Electr. Device L.*, vol. 39, no. 3, pp. 375-378, 2018.

[3] R. N. Bukke, N. N. Mude, J. Lee, C. Avis and J. Jang, "Effect of Hf Alloy in ZrO_x Gate Insulator for Solution Processed a-IZTO Thin Film Transistors," *IEEE Electr. Device L.*, vol. 40, no. 1, pp. 32-35, 2019.

[4] C.-Y. Zhao, J. Li, D.-Y. Zhong, C.-X. Huang, J.-H. Zhang, X.-F. Li et al., "Effect of La Addition on the Electrical Characteristics and Stability of Solution-Processed LaInO Thin-Film Transistors With High-*k* ZrO_2 Gate Insulator," *IEEE T. Electron Dev.*, vol. 65, no. 2, pp. 526-532, 2018.

[5] Y.-R. Lyu and T.-E. Hsieh, "A characterization on emission property of In_2O_3–SiO_2 nanocomposite thin films," *Surf. Coat. Tech.*, vol. 231, pp. 219-223, 2013.

[6] J.-W. Jo, Y.-H. Kim and J. Park, "Ultralow-Temperature Solution-Processed Aluminum Oxide Dielectrics via Local Structure Control of Nanoclusters," *ACS Appl. Mater. Inter.*, vol. 9, no. 40, pp. 35114-35124, 2017.

[7] H. S. Kim, P. D. Byrne and A. Facchetti, "High performance solution-processed indium oxide thin-film transistors," *J. Am. Chem. Soc.*, vol. 130, no. 38, pp. 12580-12581, 2008.

[8] J. H. Park, Y. B. Yoo and K. H. Lee, "Low-temperature, high-performance solution-processed thin-film transistors with peroxo-zirconium oxide dielectric," *ACS Appl. Mater. Inter.*, vol. 5, no. 2, pp. 410-7, Jan 23 2013.

[9] S.-Y. Han, M.-C. Nguyen and A. H. T. Nguyen, "Effect of Li-doping on low temperature solution-processed indium–zinc oxide thin film transistors," *Thin Solid Films*, vol. 641, pp. 19-23, 2017.

[10] D. Khim, Y. H. Lin, and S. Nam, "Modulation-Doped In_2O_3 /ZnO Heterojunction Transistors Processed from Solution," *Adv. Mater.*, vol. 29, no. 19, May 2017.

[11] L. Zhu, G. He, and Y. Long, "Eco-Friendly, Water-Induced In_2O_3 Thin Films for High-Performance Thin-Film Transistors and Inverters," *IEEE Electr. Device L.*, 2018.

[12] C. Fan, A. Liu, Y. Meng, Z. Guo, G. Liu, and F. Shan, "Solution-Processed SrO x-Gated Oxide Thin-Film Transistors and Inverters," *IEEE T Electr. Dev.*, vol. 64, no. 10, pp. 4137-4143, 2017.

[13] K. Banger, C. Warwick, J. Lang, K. Broch, J. E. Halpert, J. Socratous et al., "Identification of dipole disorder in low temperature solution processed oxides: its utility and suppression for transparent high performance solution-processed hybrid electronics," *Chem. Sci.*, vol. 7, no. 10, pp. 6337-6346, 2016.

[14] B. D. Choi, H. S. Kim, Y.-G. Ha, J. An, K. Ahn, J. Hong et al., "Solution-Processed Amorphous Zn–In–Sn–O/ZrO2 Based Field-Effect Transistors," *J Nanosci. Nanotechno.*, vol. 16, no. 11, pp. 11406-11412, 2016.

[15] C. Zhu, A. Liu, G. Liu, G. Jiang, Y. Meng, E. Fortunato et al., "Low-temperature, nontoxic water-induced high-k zirconium oxide dielectrics for low-voltage, high-performance oxide thin-film transistors," *J Mater. Chem. C.*, vol. 4, no. 45, pp. 10715-10721, 2016.

[16] Y. Hwan Hwang, J.-S. Seo, J. Moon Yun, H. Park, S. Yang, S.-H. Ko Park et al., "An ‘aqueous route’ for the fabrication of low-temperature-processable oxide flexible transparent thin-film transistors on plastic substrates," *NPG Asia Mater.*, vol. 5, no. 4, pp. e45-e45, 2013.

[17] W. Xu, M. Long, and T. Zhang, "Fully solution-processed metal oxide thin-film transistors via a low-temperature aqueous route," *Ceram. Inter.*, vol. 43, no. 8, pp. 6130-6137, 2017.

[18] J. S. Lee, Y.-J. Kwack and W.-S. Choi, "Inkjet-printed In_2O_3 thin-film transistor below 200 ℃," *ACS Appl. Mater. Inter.*, vol. 5, no. 22, pp. 11578-11583, 2013.

[19] X. Huang, J. Song and P. Lai, "Improved Stability of α-InGaZnO Thin-Film Transistor under Positive Gate Bias Stress by Using Fluorine Plasma Treatment," *IEEE Electr. Device L.*, vol. 38, no. 5, pp. 576-579, 2017.

[20] Z. Lin, Y. Liu, U. Halim, M. Ding, Y. Liu, Y. Wang et al., "Solution-processable 2D semiconductors for high-performance large-area electronics," *Nat.*, Oct 3 2018.

[21] A. Liu, H. Zhu, G. Liu, Y. Y. Noh, E. Fortunato, R. Martins et al., "Draw Spinning of Wafer-Scale Oxide Fibers for Electronic Devices," *Adv. Electr. Mat.*, vol. 4, no. 6, p. 1700644, 2018.